

# MARCHING VELOCITY OF CAPILLARY MENISCUSES IN MICROCHANNELS

Lung-Jieh Yang\*, Tze-Jung Yao, Yu-Lin Huang\*, Yong Xu and Yu-Chong Tai

Electrical Engineering, 136-93, California Institute of Technology, USA

\*Tamkang University, Taiwan ROC

[ljyang@mail.tku.edu.tw](mailto:ljyang@mail.tku.edu.tw)

## ABSTRACT

This paper describes a new method and an analytical model for characterizing the surface energy inside a microchannel using the measurement of the marching velocity of a capillary meniscus. This method is based on the fact that surface tension of a liquid meniscus in a hydrophilic case produces pressure to pull liquid into the channel and the velocity of the meniscus is related to the surface energy. Both Parylene and silicon nitride microchannels with different surface conditions were fabricated to perform the liquid-filling experiments. It is shown that our model agrees well with the data and this is a valid method.

**Keywords:** Parylene, microchannel, capillary

## INTRODUCTION

The capillary phenomena had been studied in the early period of 19<sup>th</sup> century. There's almost no new progress since then by the constraint of experimental facilities and techniques. This topic is one of microscopic dimensions in the classical mechanics [1]. The capillary phenomena can be defined quantitatively in terms of surface tension. Surface tension makes the surface of a liquid act as an elastic sheath, which minimizes the surface area of liquid so as to minimize the energy of the fluidic system minimal. Although liquid/solid contact angle method has been established for decades to measure the surface energy of a flat surface, to our knowledge there is no existing method to measure the surface properties inside a capillary tube especially in the micro domain. It is the goal of this project to develop an easy method and we propose to use the marching velocity of the meniscus front in the channel to measure the surface energy inside a microchannel.

## YOUNG'S LAW

Figure 1 shows a liquid droplet on a solid surface at steady state. There are three surface forces, including  $\gamma_{la}$ ,  $\gamma_{sl}$ , and  $\gamma_{sa}$ , acting at the liquid/solid/air interface satisfying Young's law as [2].

$$\gamma_{sa} = \gamma_{sl} + \gamma_{la} \cos \theta_c \quad (1)$$

where  $\theta_c$  is the contact angle.

## SURFACE ENERGY

From the energy perspective, the effective surface tension force applied on the fluid column can be deduced from the derivative of the surface energy of the whole fluid system with respect to the spatial coordinate. Figure 2 is the configuration of a capillary microchannel. The total surface energy of the capillary channel is composed of four parts. The first one is the vacant area ( $A_T - Ax$ ) multiplied with  $\gamma_{sa}$ . The second part is the wetting area  $Ax$  multiplied with  $\gamma_{sl}$ . The third part is the surface energy  $E_0$  stored in the filling reservoir.  $E_0$  hardly changes due to the infinitesimal amount of liquid filling into the capillary. The fourth part is the complex surface of capillary meniscus front multiplied with  $\gamma_{la}$ . We neglect the fourth term for the very small area of meniscus front compared to the other surfaces.

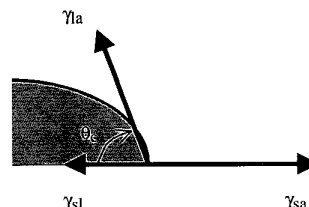


**Figure 1:** The liquid/solid/air interface of a droplet;  $\theta_c$  is the contact angle.  $\gamma_{ij}$  denotes surface tension between phase  $i$  and  $j$ .

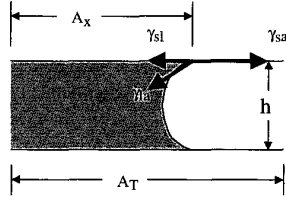


**Figure 2:** The configuration of a microchannel;  $h$  is the channel height.  $A_x$  denotes wetting area with the length of  $x$ , and  $A_T$  denotes the total area with the length of  $L$ .

Then the total energy of the capillary channel in Fig. 2 is expressed as

$$E_S = E_0 + [A_T \gamma_{sa} + A_x (\gamma_{sl} - \gamma_{sa})] \quad (2)$$

Assuming the cross section of the capillary channel in Fig. 2 is rectangular with a width of  $g$  and height of  $h$ , the total energy can be expressed as

$$E_S = E_0 + 2(h+g)[L \cdot \gamma_{sa} - x \cdot (\gamma_{sa} - \gamma_{sl})] \quad (3)$$

### (1) Capillary force

Taking the derivative of Eq. (3) with respect to  $x$ , we obtain the equivalent force  $F$  applied on the capillary fluid column along  $x$  direction.

$$F = -\frac{dE_S}{dx} = 2(h+g) \cdot (\gamma_{sa} - \gamma_{sl}) = \Delta p_{la} \cdot g \cdot h \quad (4)$$

The pressure drop across the liquid-air interface is therefore deduced under the assumption that channel height  $h$  is much smaller than channel width  $g$ .

$$\Delta p_{la} \approx \frac{2(\gamma_{sa} - \gamma_{sl})}{h} \quad (5)$$

Eq.(5) can be rewritten as the so-called ‘‘Laplace pressure drop’’ for the circular capillary tube by changing the channel characteristic length by the hydraulic diameter  $D_h (=2r_h=2r\cos\theta_c=2gh/(g+h))$ .

$$\Delta p_{la} = \frac{2(\gamma_{sa} - \gamma_{la})}{r} \quad (6)$$

where  $r$  is the radius of the capillary tube.

Laplace Eq. (6) demonstrates that the smaller the channel dimension, the larger the pressure drop across the liquid-air capillary interface.

### (2) The measurement of contact angles

To study open surface properties, the contact angle measurement is a powerful way. However, measuring the inner surface properties is much more difficult. A delicate apparatus for capturing the meniscus images in quartz capillary tubes to measure the meniscus velocity is reported by Sobolev[3], where the gas pressure, position,

velocity and dynamic contact angle of a meniscus were correlated. The measurement of the inner surface properties of a microchannel is very important for microfluidics and bioMEMS. However, the microfluidic properties are even more difficult to characterize and quantify in terms of dimensional control and applications of other parameters (e.g., pressure). This paper aims to explore a new method of measuring the marching position and velocity of a capillary meniscus in micromachined channels to interpret microfluidic properties. Experimentally, filling water into a microchannel with different surface conditions can generate a variety of marching velocities for the same liquid. The development of the one-dimensional mathematic model of Fig. 2 is based on the balance of forces between channel flow and meniscus (Laplace) pressure shown in the following description.

### (3) The velocity model of marching meniscus

Once the pressure drop of meniscus front is known, one can use the incompressible Navier-Stokes equation to derive the velocity capillary meniscus front. Treated as the one-dimensional time-variant fluid field with only the horizontal velocity variable  $u$  generally varying with the spatial coordinates and time, the instantaneous position of capillary meniscus  $L(t)$  is described as the following differential system.

Continuity equation (conservation of mass):

$$\frac{\partial u}{\partial x} = 0; (\Rightarrow u = u(y, t)) \quad (7)$$

Momentum equation (conservation of momentum):

$$\frac{\partial u}{\partial x} = -\frac{1}{\rho} \frac{dp}{dx} + \frac{\mu}{\rho} \frac{\partial^2 u}{\partial y^2}; \left( -\frac{dp}{dx} = \frac{2(\gamma_{sa} - \gamma_{sl})}{h \cdot L(t)} \right) \quad (8)$$

Position of meniscus:

$$u(0, t) = \frac{dL(t)}{dt} \quad (9)$$

Boundary condition:

$$u(h/2, t) = 0 \quad (10)$$

$$\frac{\partial u}{\partial y}(0, t) = 0 \quad (11)$$

Initial condition:

$$u(y, 0) = 0; L(0) = L_0 \quad (12)$$

The velocity variation along the  $y$ -direction is not important in this model. We substitute a parabolic distribution Eq.(13) of  $u(y, t)$ , which satisfies the non-slip boundary conditions (10) and (11) automatically, into Eq. (8). Then we obtain Eq. (14).

$$u(y, t) = u_0(t) \cdot \left[ 1 - \left( \frac{2y}{h} \right)^2 \right] \quad (13)$$

$$u_0'(t) \cdot \left[ 1 - \left( \frac{2y}{h} \right)^2 \right] + \frac{\mu}{\rho h^2} u_0(t) = \frac{2(\gamma_{sa} - \gamma_{sl})}{\rho \cdot h \cdot L(t)} \quad (14)$$

Eq. (14) basically demonstrates the force balance between the momentum of channel-flow and the meniscus (Laplace) pressure-drop. It will be inherently reasonable if we additionally take the average of it along the y-direction. Then the initial value problem (IVP) of the marching position  $L(t)$  of capillary meniscus with respect to time is

$$\left( L'' + \frac{12\mu}{\rho h^2} L' \right) \cdot L = \frac{3(\gamma_{sa} - \gamma_{sl})}{\rho h} \quad (15)$$

$$\text{I.C.: } L'(0)=0; L(0)=L_0 \quad (16)$$

Since there is no exact solution of the nonlinear IVP (15) (16), we have to solve it numerically. However, if we neglect the acceleration (2<sup>nd</sup> derivative) term of Eq. (15) which is the case in our time domain ( $t \gg \mu s$ ), then the simplified secular solution of  $L(t)$  can be regarded as the marching position following a square-root relation with time ( $D$  is a diffusing coefficient).

$$L(t) = \sqrt{L_0^2 + Dt}, \quad D = \left( \frac{h \cdot (\gamma_{sa} - \gamma_{sl})}{2\mu} \right) \quad (17)$$

## RESULTS AND DISCUSSION

Experimentally, we then fabricated a silicon chip with Parylene microchannels as shown in Fig. 3 to perform the water-filling experiment. The moving images of water meniscus for a Parylene channel with the width of  $10 \mu m$ , height of  $3 \mu m$  subjected to dried, pre-wetted and pretreated (with agents other than water) inner walls, were recorded through an optical microscope and a CCD into a VCR tape. We transformed the VCR images into digital movie files, which have a time resolution of  $1/30$  sec. Finally, information regarding the position of the moving meniscus was collected and plotted in Fig. 4. By fitting the data according to the square-root in Eq. (2), we obtained the diffusing coefficient  $D$  in Tab. 2. Clearly, the square-root dependence is valid and this model fits with the experimental data really well as shown in Fig. 4. The results shown in Tab. 2 reveal small values of the surface energy difference ( $\gamma_{sa} - \gamma_{sl}$ ) compared to the surface energy of water ( $\gamma_{fa} = 0.073$  Nt/m). This correlates to dynamic contact angles  $\theta_c$  for different cases of water meniscus in a Parylene microchannel are almost  $90^\circ$  while the diffusing coefficient  $D$

changes over 3 orders of magnitude. This water-filling observation shows the importance of sample preparation when conducting experiments on polymer surfaces. The change in Parylene surface energy with different processes is a well-known and intricate phenomenon. Processes such as photoresist spinning and stripping, plasma roughening and solvent immersion would change the surface from hydrophobic to hydrophilic completely. However, these changes sometimes can be reversed after air-drying the sample so the surface would reverse to the original surface state.

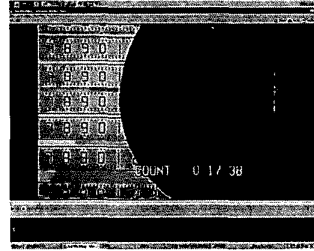


**Figure 3:** The Parylene channels of 2mm long, with the height of  $3 \mu m$ , the width of 80, 40, 20,  $10 \mu m$  (from bottom to top) on a silicon chip. Each small step of the ruler is  $20 \mu m$ . The water droplet (dark area) serves as a reservoir at inlet.

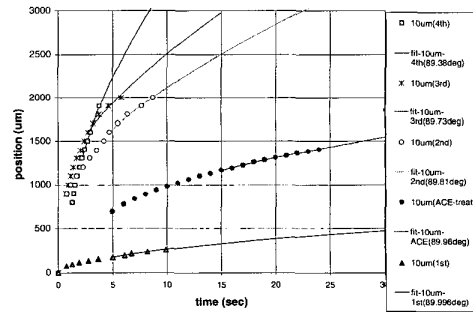


**Figure 4:** The position of a capillary meniscus vs. time of DI water filling into a Parylene channel. The fitting curves depict the theoretical prediction

### (2) The velocity variation due to different surface states

The large variation of diffusion coefficient  $D$  and the meniscus velocity in Tab. 2 can be explained by surface humidity of the Parylene micro-channel. Right after the first filling and drying, the inner Parylene surface adsorbs water molecules and is apt to conducting the next water fluid marching more easily into the micro-channel with a much higher (two

order of magnitude higher) speed. It is also interesting that the velocity shifts somewhat back to the case of the first water-filling in Tab. 1 if we treated the inner channel surface with acetone again (just as the situation of stripping away the sacrificial photo-resist).

To further test the theory developed for the water-filling experiment,  $\text{Si}_x\text{N}_y$  microchannels are also fabricated using  $0.5\mu\text{m}$  polysilicon as sacrificial layer. The sacrificial polysilicon are finally etched away using TMAH and the channels are also subjected to piranha cleaning prior to the testing. The results is shown in Fig.5. For example, the diffusion coefficient extracted from the water experiment in Fig.5 shows a surface energy difference of  $0.0395\text{Nt/m}$ . This value corresponds to the dynamic contact angle of  $57.24^\circ$  which is close to the steady-state contact angle measurement of  $45^\circ$  done on the surface of the same chip.

Thus, the fill-in experiment herein not only describes the surface tension-driven mechanism but also the surface state of a micro-channel. It may inspire another possibility of identifying the micro-channel with different generic parameters other than the geometric specification (size, roughness, etc.) on micrometer scale. In other words, by performing the filling experiment of the working liquid and recording the marching velocity of capillary meniscus, more precise information can be gathered to identify micro-fluidic parameters for applications such as micro-cooling and micro-injection.

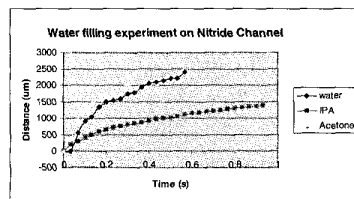


**Figure 5:** The position of a capillary meniscus vs. time of different liquids filling into a silicon nitride microchannel.

## CONCLUSION

This paper introduced a method to measure the surface energy difference of a moving capillary meniscus in a micro-channel. The measured velocity data subjected to different surface states varies across three orders of

magnitude. With the experimental methodology developed in this paper, the mechanism of the surface tension-driven flow becomes more apparent and can be applied to fluid-delivery of microfluidic systems. Further development of this technique will facilitate collection of essential surface property data for further understanding of the microchannel flow.

**Table 1:** The experiment results.

	Diffusing coefficient $D$ ( $\mu\text{m}^2/\text{sec}$ )	Surface Energy Difference $(\gamma_{sa} - \gamma_{sl}) \text{ Nt/m}$
A	68450	$3.51 \times 10^{-5}$
B	7584	$3.89 \times 10^{-6}$
C	361500	$1.85 \times 10^{-4}$
D	514300	$2.637 \times 10^{-4}$
E	1177000	$6.036 \times 10^{-4}$

- (A) Pre-treated with acetone for three times before filling water
- (B) 1<sup>st</sup> time of filling water after stripping PR (dried capillary)
- (C) 2<sup>nd</sup> time of filling water (pre-wetted capillary)
- (D) 3<sup>rd</sup> time of filling water
- (E) 4<sup>th</sup> time of filling water

## ACKNOWLEDGEMENT

The authors want to thank the helps from Dr. Xing Yang and Mr. Ken Walsh of the Caltech Micromachining group. This project is also partially supported by the NSF Engineering Research Center for Neuromorphic Systems Engineering (CNSE) at Caltech and National Science Foundation (NSC) from Taiwan, R.O.C.

## REFERENCES

- [1] M. Madou, Fundamentals of microfabrication, CRC, p.433, 1997.
- [2] J.N. Israelachvili, Intermolecular and Surface Forces, London: Academic, 1992.
- [3] V.D. Sobolev, J. Colloid and Interface Science, 222, pp.51-54, 2000
- [4] P.G. de Gennes, Reviews of Modern Physics, 57(3-1), pp.827-890, 1985.